Vibrational properties of $LaPO_4$ nanoparticles in mid- and far-infrared domain

P. Savchyn,[1] I. Karbovnyk,[2,a)] V. Vistovskyy,[1] A. Voloshinovskii,[1] V. Pankratov,[3] M. Cestelli Guidi,[4] C. Mirri,[4] O. Myahkota,[5] A. Riabtseva,[5] N. Mitina,[5] A. Zaichenko,[5] and A. I. Popov[3,6]

[1]*Department of Physics, Ivan Franko National University of Lviv, 8 Kyrylo & Mefodii Str., 79005 Lviv, Ukraine*
[2]*Department of Electronics, Ivan Franko National University of Lviv, 107 Tarnavskogo Str., 79017 Lviv, Ukraine*
[3]*Institute of Solid State Physics, University of Latvia, 8 Kengaraga, LV-1063 Riga, Latvia*
[4]*INFN-Laboratori Nazionali di Frascati, 40 Via E. Fermi, 00044 Frascati, Italy*
[5]*Lviv Polytechnic National University, 12 S. Bandera Str., 79013 Lviv, Ukraine*
[6]*Institute Laue–Langevin, BP 156, 38042 Grenoble Cedex 9, France*

(Received 8 July 2012; accepted 19 November 2012; published online 19 December 2012)

Nanopowders of $LaPO_4$ have been grown by sedimentation-micellar method. As-prepared $LaPO_4$ nanoparticles with the average grain size of about 8 nm have a single-phase hydrated hexagonal structure. After thermal annealing at 600 and 800 °C, the average size of nanoparticles increases up to ~35 and ~50 nm, respectively, and the structure transforms into single-phase monoclinic. IR spectra of $LaPO_4$ nanoparticles of different size were investigated in the wide range of wavenumbers from 130 to 5000 cm^{-1} in the 20–300 K temperature region. Differences between IR spectra of the bulk material and nanoparticles as well as the temperature behavior of the vibrational properties are discussed. © *2012 American Institute of Physics*. [http://dx.doi.org/10.1063/1.4769891]

I. INTRODUCTION

Lanthanum orthophosphate ($LaPO_4$), also known as monazite, has been widely used as a green phosphor, when doped with Ce^{3+} and Tb^{3+} in high-quality tricolour luminescent lamps.[1] It has been used as a proton conductor, as well as in lasers, sensors, ceramic materials, catalysts, and heat-resistant materials. This is due to its interesting properties, such as high thermal stability, very low solubility in water, high index of refraction, and so on.[1–5] $LaPO_4$ also exhibits quite a good ionizing and particle radiation as well as photochemical stability and thus it has been also suggested as a prospective waste form for high-level nuclear waste.[6,7]

In recent years, $LaPO_4$ has been also shown to be a useful host lattice for lanthanide ions to produce phosphors that emit in a broad range of colors.[1,5,8–10] Doping with different types of rare earth ions (Eu^{3+}, Ce^{3+}, Tb^{3+}, Nd^{3+}, Er^{3+}, Pr^{3+}, Ho^{3+}, Yb^{3+}, Tm^{3+}) of macro- as well as nanosized $LaPO_4$ has been frequently reported in the literature.[11–14]

Recently, considerable attention was paid to the synthesis and investigation of $LaPO_4$ nanoparticles doped by different rare-earth ions. Typical examples of such objects are nanocrystals,[8,9,15–18] nanorods,[13] nanofibers,[12] etc. This kind of nanoparticles produces efficient luminescence in visible or near-IR range depending upon impurity rare-earth ion. Therefore, they are considered as promising materials for lighting phosphors and optical amplification materials in telecommunications.[5] Another promising application of $LaPO_4$ nanoparticles is concerned with the creation of luminescence labels for biomedical testing. These labels are based on luminescent nanoparticles coated by a polymer shell or by the same undoped or other inorganic material.[19,20] Therefore, most studies of these nanoparticles are concerned with luminescence properties.

Lanthanum phosphate is known to crystallize in two possible structures: hexagonal hydrated rhabdophane type $LaPO_4 \cdot H_2O$ (space group is $P6_222$ with three molecular units per unit cell) or monoclinic anhydrous monazite type $LaPO_4$ (space group is $P12_1/n1$ with four formula units per unit cell).[21,22] In the latter structure, both La and PO_4 ions are located in general C_1 sites.[23] Space group $P6_222$ provides sets of three-fold sites with point symmetry D_2 for metal and phosphate ions, and six-fold sites with point symmetry C_2 for phosphate,[21] while water molecules occupy C_1 sites.[24]

According to Hezel and Ross,[23] a common feature of the vibrational spectra of $LaPO_4$ is the internal modes of the PO_4 group (point symmetry C_1 for monoclinic and C_2 for hexagonal $LaPO_4$). No selection rules apply for such symmetry and all possible combinations of fundamental vibrations should be IR active.

Vibrational spectra of nanoparticles generally differ from those of respective bulk materials[25,26] due to quantum confinement effect and size effect,[25,27] interfacial effect,[28] surface amorphousness, and high internal stress.[29] From all the above reports, the important conclusion is that the optical absorption and scattering in the fundamental lattice absorption region should be size-dependent.

There are a number of reports where vibrational properties of $LaPO_4$ obtained in different forms (bulk, powders) and under various synthesis conditions were investigated both by FTIR and Raman spectroscopy. However, the dependence of vibrational frequencies on the size of $LaPO_4$ nanoparticles has not been established definitively. Therefore, the modification of the phonon spectra for different kind of $LaPO_4$ nanoparticles is still an open question and our

a)Author to whom correspondence should be addressed. Electronic mail: ivan_karbovnyck@yahoo.com.

aim is to study the vibrational spectra of $LaPO_4$ nanoparticles with different average size, both pure and doped with Eu ions (~5%) and, at the same time, macro-sized $LaPO_4$ as a reference in the mid- and far-IR domain utilizing FTIR spectroscopy. In particular, we focus on establishing the influence of quantum confinement, surface effects, and polymer coating on the low energy phonon spectra of different $LaPO_4$ nanoparticles.

Various solution-phase routes, including combustion,[30] sol-gel,[31,32] precipitation,[33] water-oil microemulsion,[34] polyol-mediated process,[35] ultrasonification,[36] hydrothermal,[37,38] and mechanochemical method,[39] have been used to obtain high-quality $LaPO_4$-based nanoparticles.

However, the simple and mass fabrication of $LaPO_4$ nanoparticles with narrow grain size distribution and uniform morphology still remains an important challenge. In this paper, we have used the sedimentation-micellar method, which is described in Sec. II.

II. EXPERIMENTAL

A. Samples synthesis

The powders of $LaPO_4$ have been obtained by sedimentation-micellar method using the water solutions of the corresponding salts. $LaPO_4$ nanoparticles were synthesized using well known technique from water solutions of corresponding salts.[40] Control of the nanoparticles size and tailored functionalization of their surface were performed using novel functional surface-active oligoperoxide[41,42] as micelle-forming template and surface modifier during their nucleation. For this purpose, $LaCl_3 \cdot 7H_2O$ aqueous solution has been prepared. $EuCl_3$ solution was added to the previous one in the mass ratio of 1 to 0.035 in the case of $LaPO_4$-Eu nanoparticles preparation. Separately, the ricinox batch was dissolved in water (5 mass %). Small amount (with respect to lanthanum chloride) of $NaH_2PO_4 \cdot 2H_2O$ was added to the ricinox solutions and stirred until dissolved. Eventually, a finely dispersed white precipitate was obtained.

The precipitate was isolated by centrifugation and repeatedly washed with distilled water and ethanol. The obtained nanoparticles were exposed to annealing at 600 and 800 °C during 2 h in order to receive the larger sizes. Annealing of $LaPO_4$ nanoparticles leads to dehydration and changes in core crystal structure from hexagonal to monoclinic. Consequently, one observes a substantial increase of the size of nanoparticles.

We carried out surface modification of nanoparticles $LaPO_4$ via controlled adsorption by oligoperoxide AR-2. The oligoperoxide is copolymer of N-vinyl pyrrolidone, unsaturated peroxide 2-tertbutylperoxy-2-methyl-5-hexene-3-yne, and glycidyl methacrylate of a structure

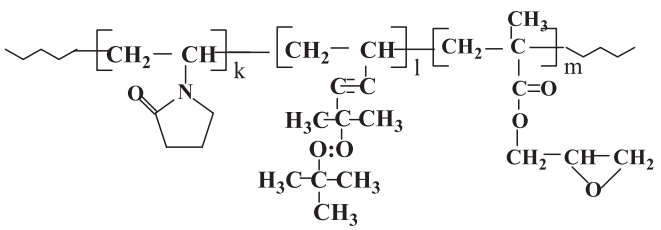

where k = 70.80%, l = 14.72%, m = 14.48%, and molar mass M = 3000 g/mol. It was synthesized via solution polymerization by the procedure described in Ref. 43.

For surface modification, we used the nanoparticles formed by annealing at 800 °C. The acetone dispersion of nanoparticles (1 g in 5 ml) was mixed with solution of acetone oligoperoxide. The process was performed with a mixing at room temperature in order to achieve equilibrium adsorption of oligoperoxide. To clear the samples from unbound oligoperoxide, repeated washing with acetone was exploited. The oligoperoxide coating thickness was about 20 nm.

For X-ray diffraction studies, the uniform layer of nanopowders was deposited on a substrate using X-ray-amorphous glue. The diffraction patterns were obtained by means of STOE STADI IP diffractometer. Nanoparticle size was determined using Debye-Scherrer equation

$$a = \frac{K\lambda}{B\cos\theta},$$

where K is the shape factor (the dimensionless shape factor has a typical value of about 0.9), λ is the X-ray wavelength, B is the line broadening at half the maximum intensity (FWHM) in radians, and θ is the Bragg angle.

After synthesis, the nanoparticles of single-phase hydrated hexagonal $LaPO_4$ (space group $P6_222$) was obtained with the following unit cell parameters: $a = 7.152(18)$, $c = 6.434(15)$ Å; average size of grains was 8 nm. After dehydration by thermal annealing, particles were single-phase (space group $P12_1/n1$) and lattice parameters and grain sizes were depending on annealing temperature. After annealing at 600 °C, average size of grains was 35 nm and the lattice parameters were $a = 6.8437(2)$, $b = 7.07843(17)$, $c = 6.51434(16)$ Å, $\beta = 103.3105(19)°$. After annealing at 800°C, average size of grains was 50 nm and the lattice parameters were $a = 6.84250(7)$, $b = 7.07956(6)$, $c = 6.51229(6)$ Å, $\beta = 103.2688(7)°$. It has to be noted that the all lattice parameters of monoclinic bulk $LaPO_4$ are significantly smaller: $a = 6.825(4)$, $b = 7.057(2)$, $c = 6.482(2)$Å, $\beta = 103.21(4)°$ as given in Ref. 44 or $a = 6.835$ Å, $b = 7.070$ Å, $c = 6.503$ Å, $\beta = 103.23°$ as given in Ref. 39, for example.

Commercial macro-size $LaPO_4$ powder from Philips (with the average size of grains of ~10 μm) was used as a reference.

B. Measurements

IR spectroscopy was performed at infrared beamline SINBAD of Daphne Light synchrotron IR facility, which is described in Ref. 45 and intensively used for nondestructive quantitative characterization of different types of the micro- and nanomaterials.[46–51]

At the DAΦNE-Light Laboratory, the IR radiation is extracted from a bending magnet of the electron ring and transmitted to an interferometer at a distance of about 25 m using a beam line kept under ultra-high vacuum up to a diamond window placed at the entrance of the spectrometer. The instrument used was BRUKER Equinox 55, modified to work in a low-vacuum regime in the whole IR range down to

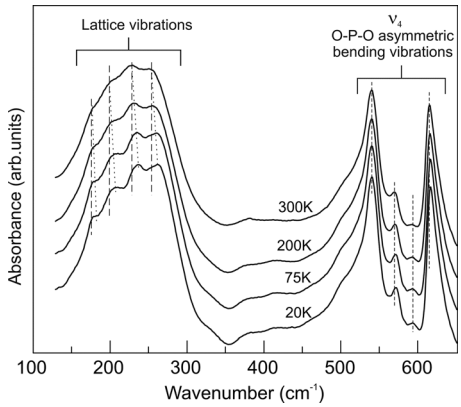

FIG. 1. FIR spectra of hydrated hexagonal $LaPO_4$ nanoparticles with average size of about 8 nm at different temperatures.

the far-IR domain.[45] Experiments were performed in a vacuum of about 10^{-2} mbar in transmission mode at temperature from 300 K down to 20 K with a step of 50 K.

All the samples used for FTIR analysis were prepared in the form of pellets after mixing with a commercial CsI powder of 99.995% purity. FIR and MIR spectra for all samples were recorded in the spectral ranges of 130–650 cm^{-1} and 400–5000 cm^{-1}, respectively, with the spectral resolution of 0.5 cm^{-1}.

III. RESULTS AND DISCUSSION

The results of performed measurements are presented in Figs. 1–4.

First, vibrational spectra of hydrated hexagonal $LaPO_4$ nanoparticles with the average size of about 8 nm were analyzed. These spectra recorded at different temperatures are shown in Fig. 1 (FIR domain) and Fig. 2 (MIR domain). There are three main groups of vibrational bands, attributed to lattice vibrations and the PO_4 group[23,24,52,53] (observable both in Figs. 1 and 2), and some additional bands at higher wavenumbers up to 4000 cm^{-1}, related to water and other technological components remained after $LaPO_4$ synthesis (see Fig. 2).

The first group consists of four broad and poorly resolved bands at about 178, 202, 228, and 253 cm^{-1} (positions are given at 300 K). At decreasing temperatures, these bands become sharper and their positions are shifted to higher energies by approximately 8–9 cm^{-1} at 20 K as evident from Fig. 1. Such temperature shift of vibrational frequencies can be caused by the thermal expansion of the lattice.[54,55]

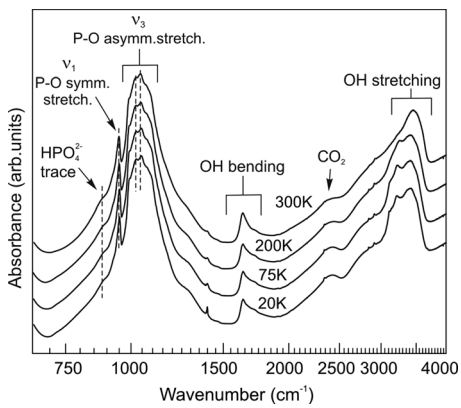

FIG. 2. MIR spectra of hydrated hexagonal $LaPO_4$ nanoparticles with average size of about 8 nm at different temperatures.

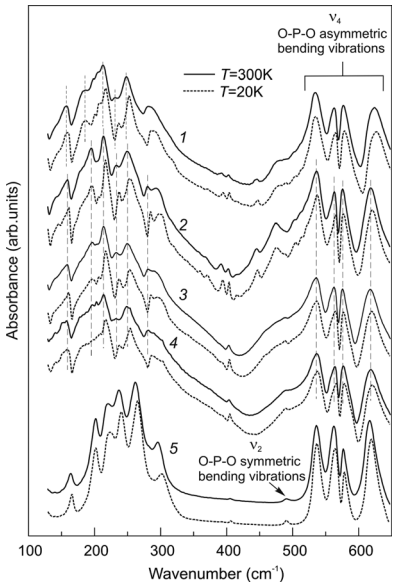

FIG. 3. FIR spectra of monoclinic $LaPO_4$ samples with different average size of particles: (*1*) 35 nm, (*2–4*) 50 nm (*3*) $LaPO_4$-Eu, (*4*) $LaPO_4$-Eu+ oligoperoxide), (*5*) macro-sized.

In the MIR domain (see Fig. 2) for hexagonal $LaPO_4$, the sharp peak at 1640 cm^{-1} and the broad band at 3460 cm^{-1} are observed. The latter splits in two bands (3220 and 3440 cm^{-1}) at lower temperatures. Both 1640 cm^{-1} and 3460 cm^{-1} bands can be ascribed to coordinated water due

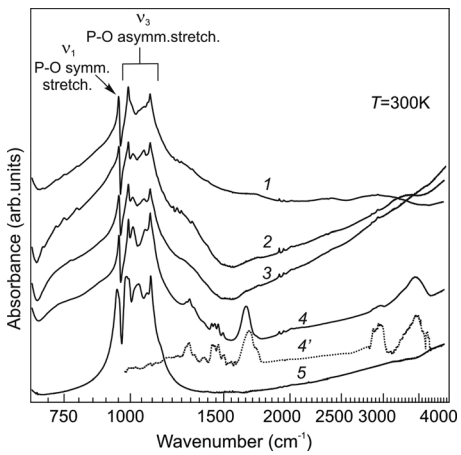

FIG. 4. MIR spectra of monoclinic $LaPO_4$ samples with different average size of particles: (*1*) 35 nm; (*2–4*) 50 nm (*3*) $LaPO_4$-Eu; (*4*) $LaPO_4$-Eu+ oligoperoxide; (*4′*) oligoperoxide); (*5*) macro-size.

to the following. Hexagonal phosphates are hydrated as confirmed by the appearance of strong absorption bands in the IR spectra.[24] Hexagonal structure of $LaPO_4 \cdot nH_2O$ is built of PO_4 tetrahedra and LaO_8 polyhedra connected together and it forms the chains which are linked by the P–O–La bonds leaving an open channels along the hexagonal *c* axis. These channels could be occupied by the water molecules which would stabilize the structure.[22] So, the bands located near 3460 cm^{-1} can be attributed to O–H stretching modes, while the bending modes are at around 1630 cm^{-1}.[24,57,58] These bands are not observed for monoclinic orthophosphates indicating loss of zeolite water during heating the sample. The absence of water vibration band in the 700–800 cm^{-1} range indicates zeolitic nature of water.[59–61] One can see a broad band above 3000 cm^{-1}, which is adjacent to the water vibrational bands and possibly can be attributed to the surface P-OH bonds.[62]

Very weak shoulder near 885 cm^{-1} (indicated by dotted vertical line in Fig. 2) can be ascribed to the presence of HPO_4^{2-} trace in these nanoparticles from acidic solution (NaH_2PO_4) where HPO_4^{2-} for PO_4^{3-} is possible. The absence of this shoulder in the spectra of other samples may be due to the decomposition of HPO_4^{2-} upon ignition at high temperatures.[63,64]

Weak band around 2420 cm^{-1} (see Fig. 2) is very likely a manifestation of CO_2 (similar feature has been reported for $LaPO_4:Eu^{3+}$ in Ref. 65). Upon increasing the synthesis temperature, this band diminishes as the carbon dioxide is removed from the material.

With the transition of the hydrated $LaPO_4$ into monoclinic anhydrous type upon annealing the structure of absorption spectra in the range of 130–650 cm^{-1} become more pronounced with a larger number of bands. Spectra recorded for different samples show good resemblance (see Fig. 3, *curves 1–4*). It should be noted that no significant influence of Eu-impurity and modification of nanoparticles with oligoperoxide is detected (*curves 2–4*). Eu ions replace La atoms in the structure of $LaPO_4$.[66] Taking into account the small difference of ionic radii (103.2 pm for La^{3+} and 94.7 for Eu^{3+} (Ref. 67)) and low concentration of incorporated Eu, we do not expect to observe a pronounced effect of Eu on the vibrational modes within the reported frequency range.

We can see also that the vibrational bands of monoclinic nanoparticles split and shift towards lower energies as compared to the respective bands of macro-size particles. However, in Ref. 25, the high-energy shift of vibrational frequencies for nanoparticles with respect to the bulk is reported. We tend to think that in our case the effect may be due to the differences in lattice parameters. In particular, unit cell parameters for bulk $LaPO_4$ mentioned above are smaller than those in case of nanoparticles. Moreover, the change of unit-cell volume is the dominant mechanism for the tendency of the vibrational bands splitting for $LaPO_4$ nanoparticles.[68]

Energy shift of vibrational frequencies of micro-sized particles with temperature is also observed. This energy shift is approximately 2–4 cm^{-1} with the temperature decrease from 300 to 20 K (see Fig. 3). It can be caused by the smaller thermal expansion of the monoclinic lattice $LaPO_4$ comparing with the expansion of the hexagonal lattice.

Temperature annealing of the nanoparticles at 600 and 800 C causes their dehydration and the bands related to the water molecules are not apparent (see Fig. 3, *curves 1–3*). Only if the surface of annealing nanoparticles were modified by the water molecules contained in the oligoperoxide, these bands appear again (see Fig. 3, *curve 4*). Also, in this case, there are additional bands in the range of 1270–1520 cm^{-1} and one can distinguish at least eight bands: 1276, 1293, 1320, 1374, 1424, 1443, 1465, and 1495 cm^{-1} and near 2960 cm^{-1}. These bands are attributed to vibrational modes of oligoperoxide, as it is shown at Fig. 4, *curve 4*.

Most of the other bands are typical for the vibrations of phosphate groups.[23,24] Free $(PO_4)^{3-}$ ion has four normal modes of vibration of a tetrahedral ion. These are ν_1 (P–O symmetric stretching), ν_3 (P–O asymmetric stretching), and ν_2 and ν_4 (O–P–O symmetric and asymmetric bending vibrations, respectively).[23,24,53,56] One has to mention that neither Eu-impurity nor oligoperoxide affects the structure and position of these bands (see Fig. 3 and 4, *curves 2–4*). Moreover, for the monoclinic $LaPO_4$, the ν_2 modes at about 491 cm^{-1} can be observed to some extent. There also appears a weak doublet near 400 cm^{-1} (see Fig. 3). As shown in Ref. 52, based on the factor group analysis and Raman data interpretation, it can be unambiguously assigned as a B_g mode and an A_g mode.

Next, we have examined the behavior of these bands with the change of particle sizes. The result is demonstrated in Fig. 5. In the ν_4 region, there are four bands for all monoclinic samples. They appear as two well-defined doublets, as depicted in Fig. 5 (*left*). In our case, the upper doublet is split around 40 cm^{-1} and the lower doublet splits by around 26 cm^{-1} with respect to macro-sized particles. With the decreasing of the particle size, the ν_4 interval slightly expands (mainly towards higher energies) and the corresponding splits increase to 42 and 27 cm^{-1} for the particles with size of 50 nm and to 47 and 31 cm^{-1} for 35 nm. It should be mentioned that with decreasing temperature (down to 20 K), this split is slightly ($\sim$1 cm^{-1}) increased. But, the

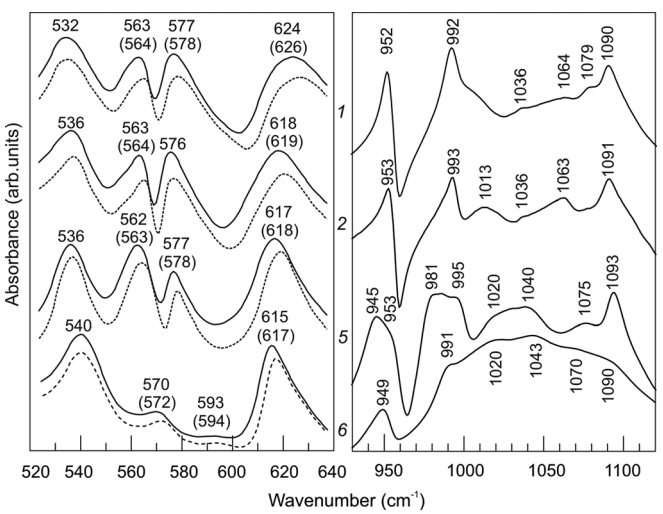

FIG. 5. Dependence of the absorption structure in the regions of ν_4 (*left; solid line* – 300 K, *dashed line* – 20 K), ν_1 and ν_3 (*right*) modes at 300 K on average size of particles: (*1*) 35 nm, (*2*) 50 nm, (*5*)–macro-sized and (*6*)–8 nm.

lowest-energy band of ν_4 does not depend on temperature and the highest-energy band shifts by 1–2 cm^{-1} towards higher energy, as shown at Fig. 5 on the left.

Lower size nanoparticles exhibit higher resonant frequency and the neighbouring vibrational bands overlap to a greater extent than the large nano- and macrosize particles. Therefore, the components of the doublets are hardly resolved (see *curve 6* in Fig. 5). As the size of the particle increases, the resolution of the vibrational bands is better resolved and the components of the doublet can be more clearly seen (*curves 1*, *2*, and *5* in Fig. 5). Qualitatively, this is observed as variations of split size and small peak shifts.

In case of the hydrated hexagonal $LaPO_4$ (see Fig 5, *curve 6*), the lowest temperature spectrum allows to resolve four bands (540, 570, 593, and 615 cm^{-1}), similarly to monoclinic $LaPO_4$. But, the frequency interval is smaller. The authors of Refs. 39 and 60, for example, have reported that ν_4 appears as a triplet (542, 569, and 617 cm^{-1} (Ref. 39) or 542, 570, and 615 cm^{-1} (Ref. 60)), while the weak band at 593 cm^{-1} could not be resolved from the data presented in these reports.

The ν_1 mode (P–O symmetric stretching) is well resolved and observed for both hexagonal and monoclinic particles (see Fig. 5, *right*). Further, a strong asymmetric stretching band ν_3 appears in the 945–1100 cm^{-1} region. Similar spectra were observed by different authors[39,56,59,60,63] and an attempt to explain their origin was made in Ref. 53. As one can see, the band of ν_3 mode is broad and not fully resolved, especially for hydrated hexagonal particles. In addition, we found a significant splitting (about 8 cm^{-1}) of ν_1 mode for micro-sized particles (a doublet around 950 cm^{-1}, *curve 5*). Splitting is observed only for largest particles and one can suggest that for nanosized particles, the components of the doublet are totally overlapped. Size effect is manifested in the displacement ($\sim$3 cm^{-1}) of peaks ascribed to ν_1 and ν_3 modes to lower energies part with decreasing particle size.

IV. CONCLUSIONS

$LaPO_4$ nanoparticles of different size and structures were synthesized and thoroughly characterized by FTIR spectroscopy.

IR spectra of hexagonal $LaPO_4$ nanoparticles exhibit four very broad and poorly resolved bands (about 178, 202, 228, and 253 cm^{-1} at 300 K) assigned to lattice modes. These bands are shifted to higher energies by approximately 8–9 cm^{-1} as temperature goes down to 20 K. Less pronounced temperature energy shift is observed for the lattice modes of monoclinic $LaPO_4$ (2–4 cm^{-1} with temperature change from 300 to 20 K). Such behavior is probably related to smaller thermal expansion of monoclinic lattice comparing with the hexagonal one.

Size dependence of vibrational modes of monoclinic $LaPO_4$ is complicated and manifests in several effects, including band splitting and energy shifts. IR bands shifts are found to be correlated with the change of lattice parameters.

Vibrational modes of the monoclinic $LaPO_4$ are influenced neither by Eu impurity nor by oligoperoxide modification.

ACKNOWLEDGMENTS

The experiments at LNF Frascati leading to these results have received funding from the European Community's Seventh Framework Programme (FP7/2007–2013) under Grant Agreement No. 226716.

The research of Lviv team was also supported by 7th FP INCO.2010-6.1 Grant Agreement No. 266531 (project acronym SUCCESS).

The work of V. Pankratov was granted by ESF Project No. 2009/0202/1DP/1.1.1.2.0/09/APIA/VIAA/141.

The research of A. I. Popov was partially supported by Sadarbıbas Projects No. 10.0032 as well as by ERAF Project No. 2010/0272/2DP/2.1.1.1.0/10/APIA/VIAA/088.

[1]N. Hashimoto, Y. Takada, K. Sato, and S. Ibuki, J. Lumin. **48–49**, 893 (1991).
[2]T. Norby and N. Christiansen, Solid State Ionics **77**, 240 (1995).
[3]Y. Hikichi, T. Ota, K. Daimon, T. Hattori, and M. Mizuno, J. Am. Ceram. Soc. **81**, 2216 (1998).
[4]Y. Fang, A. Xu, R. Song, H. Zhang, L. You, J. C. Yu, and H. Liu, J. Am. Chem. Soc. **125**, 16025 (2003).
[5]C. Feldmann, T. Jüstel, C. R. Ronda, and P. J. Schmidt, Adv. Funct. Mater. **13**, 511 (2003).
[6]G. J. McCarthy, W. B. White, and D. E. Pfoertsch, Mater. Res. Bull. **13**, 1239 (1978).
[7]A. Meldrum, L. A. Boatner, and R. C. Ewing, Phys. Rev. B **56**, 13805 (1997).
[8]K. Riwotzki, H. Meyssamy, H. Schnablegger, A. Kornowski, and M. Haase, Angew. Chem., Int. Ed. **40**, 573 (2001).
[9]S. Heer, O. Lehmann, M. Haase, and H. U. Güdel, Angew. Chem., Int. Ed. **42**, 3179 (2003).
[10]K. Riwotzki, H. Meyssamy, A. Kornowski, and M. Haase, J. Phys. Chem. B **104**, 2824 (2000).
[11]C.-H. Huang, T.-M. Chen, and B.-M. Cheng, Inorg. Chem. **50**, 6552 (2011).
[12]Z. Hou, L. Wang, H. Lian, R. Chai, C. Zhang, Z. Cheng, and J. Lin, J. Solid State Chem. **182**, 698 (2009).
[13]X. Wang and M. Gao, J. Mater. Chem. **16**, 1360 (2006).
[14]M. Yang, H. You, K. Liu, Y. Zheng, N. Guo, and H. Zhang, Inorg. Chem. **49**, 4996 (2010).
[15]V. Pankratov, A. I. Popov, S. A. Chernov, A. Zharkouskaya, and C. Feldman, Phys. Status Solidi B **247**, 2252 (2010).
[16]V. Pankratov, A. I. Popov, A. Kotlov, and C. Feldmann, Opt. Mater. **33**, 1102 (2011).
[17]V. Pankratov, A. I. Popov, L. Shirmane, A. Kotlov, and C. Feldmann, J. Appl. Phys. **110**, 053522 (2011).
[18]G. Stryganyuk, D. M. Trots, A. Voloshinovskii, T. Shalapska, V. Zakordonskiy, V. Vistovskyy, M. Pidzyrailo, and G. Zimmerer, J. Lumin. **128**, 355 (2008).
[19]C. Louis, R. C. Bazzi, A. Marquette, J. Bridot, S. Roux, G. Ledoux, B. Mercier, L. Blum, P. Perriat, and O. Tillement, Chem. Mater. **17**, 1673 (2005).
[20]J. Shen, L.-D. Sun, and C.-H. Yan, Dalton Trans. **42**, 5687 (2008).
[21]R. C. L. Mooney, J. Chem. Phys. **16**, 1003 (1948).
[22]R. C. L. Mooney, Acta Crystallogr. **3**, 337 (1950).
[23]A. Hezel and S. D. Ross, Spectrochim. Acta **22**, 1949 (1966).
[24]H. Assaaoudi, A. Ennaciri, and A. Rulmont, Vib. Spectrosc. **25**, 81 (2001).
[25]M. Thomas, S. K. Ghosh, and K. C. George Mater. Lett. **56**, 386 (2002).
[26]*Handbook of Nanostructured Materials and Nanotecnology*, edited by H. Nalwa (Academic, New York, 2000), Vol. 2, p. 90.
[27]J. Lu, H. Yang, B. Liu, and G. Zon, Mater. Res. Bull. **34**, 2109 (1999).
[28]C. Mo, Z. Yuan, L. Zhang, and C. Xie, Nanostruct. Mater. **2**, 47 (1993).
[29]M. Abdulkhadar and K. C. George, Solid State Commun. **84**, 603 (1992).
[30]M. T. Colomer, S. Gallini, and J. R. Jurado, J. Eur. Ceram. Soc. **27**, 4237 (2007).
[31]J. M. Nedelec, C. Mansuy, and R. Mahiou, J. Mol. Struct. **651**, 165 (2003).
[32]K. Rajesh, P. Shajesh, O. Seidel, P. Mukundan, and G. K. Warrier, Adv. Funct. Mater. **17**, 1682 (2007).
[33]S. Gallini, J. R. Jurado, and M. T. Colomer, J. Eur. Ceram. Soc. **25**, 2003 (2003).

[34]Y. Guo, P. Woznicki, and A. Barkatt, J. Mater. Res. **11**, 639 (1996).
[35]C. Feldmann, Adv. Funct. Mater. **13**, 101 (2003).
[36]S. S. Brown, H. J. Im, A. J. Rondinone, and S. Dai, J. Colloid Interface Sci. **292**, 127 (2005).
[37]Y. Fujishiro, H. Ito, T. Sato, and A. Okuwaki, J. Alloys Compd. **252**, 103 (1997).
[38]B. Yan and X. Xiao, Nanoscale Res. Lett. **5**, 1962 (2010).
[39]J. A. Diaz-Guillen, A. F. Fuentes, S. Gallini, and M. T. Colomer, J. Alloys Compd. **427**, 87 (2007).
[40]A. A. Hanna, S. M. Mousa, G. M. Elkomy, and M. A. Sherief, Eur. J. Chem. **1**, 211 (2010).
[41]A. Zaichenko, O. Shevchuk, V. Samaryk, and S. Voronov, J. Colloid Interface Sci. **275**, 204 (2004).
[42]A. Zaichenko, I. Bolshakova, N. Mitina, O. Shevchuk, A. Bily, and V. Lobaz, J. Magn. Magn. Mater. **289**, 17 (2005).
[43]A. Zaichenko, S. Voronov, A. Kuzaev, O. Shevchuk, and V. Vasiliev, J. Appl. Polym. Sci. **70**, 2449 (1998).
[44]D. F. Mullica, W. O. Milligan, and D. A. Grossie, Inorg. Chim. Acta **95**, 231 (1984).
[45]M. Cestelli Guidi, M. Piccinini, A. Marcelli, A. Nucara, P. Calvani, and E. Burattini, J. Opt. Soc. Am. A **22**, 2810 (2005).
[46]P. Innocenzi, T. Kidchob, J. M. Bertolo, M. Piccinini, M. Cestelli Guidi, and A. Marcelli, J. Phys. Chem. B **110**, 10837 (2006).
[47]C. Balasubramanian, S. Bellucci, G. Cinque, A. Marcelli, M. Cestelli Guidi, M. Piccinini, A. Popov, A. Soldatov, and P. Onorato, J. Phys.: Condens. Matter **18**, S2095 (2006).
[48]I. Bolesta, S. Velgosh, Y. Datsiuk, I. Karbovnyk, V. Lesivtsiv, T. Kulay, A. I. Popov, S. Bellucci, M. Cestelli Guidi, and A. Marcelli, Radiat. Meas. **42**, 851 (2007).
[49]S. Bellucci, A. I. Popov, C. Balasubramanian, G. Cinque, A. Marcelli, I. Karbovnyk, V. Savchyn, and N. Krutyak, Radiat. Meas. **42**, 708 (2007).
[50]A. Voloshynovskii, P. Savchyn, I. Karbovnyk, S. Myagkota, M. Cestelli Guidi, M. Piccinini, and A. I. Popov, Solid State Commun. **149**, 593 (2009).
[51]I. Karbovnyk, S. Piskunov, I. Bolesta, S. Bellucci, M. Cestelli Guidi, M. Piccinini, E. Spohr, and A. I. Popov, Eur. Phys. J. B **70**, 443 (2009).
[52]G. M. Begun, G. W. Beall, L. A. Boatner, and W. J. Gregor, J. Raman Spectrosc. **11**, 273 (1981).
[53]E. N. Silva, A. P. Ayala, I. Guedes, C. W. A. Paschoal, R. L. Moreira, C.-K. Loong, and L. A. Boatner, Opt. Mater. **29**, 224 (2006).
[54]P. Mogilevsky, E. E. Boakye, and R. S. Hay, J. Am. Ceram. Soc. **90**, 1899 (2007).
[55]K. H. Kim, J. Y. Gu, H. S. Choi, G. W. Park, and T. W. Noh, Phys. Rev. Lett. **77**, 1877 (1996).
[56]L. Macalik, P. E. Tomaszewski, A. Matraszek, A. Szczygieł, P. Solarz, P. Godlewska, M. Sobczyk, and J. Hanuza, J. Alloys Compd. **509**, 7458 (2011).
[57]M. F. M. Zawrah and A. A. El Kheshen, Br. Ceram. Trans. **101**, 71 (2002).
[58]R. Lemus, J. Mol. Spectrosc. **225**, 73 (2004).
[59]M. Ferhi, K. Horchani-Naifer, and M. Ferid, J. Lumin. **128**, 1777 (2008).
[60]S. Lucas, E. Champion, D. Bregiroux, D. Bernache-Assollant, and F. Audubert, J. Solid State Chem. **177**, 1302 (2004).
[61]S. Lucas, E. Champion, D. Bregiroux, D. Bernache-Assollant, and F. Audubert, J. Solid State Chem. **177**, 1312 (2004).
[62]J. W. Stouwdam, "Lanthanide-doped nanoparticles as the active optical medium in polymer-based devices," thesis (Ijsselmuiden, 2004), 159 p.
[63]R. Kijkowska, E. Cholewka, and B. Duszak, J. Mater. Sci. **38**, 223 (2003).
[64]W. W. Rudolph, Dalton Trans. **39**, 9642 (2010).
[65]G. Phaomei R. S. Ningthoujamb, W. Rameshwor Singh, N. Singh; M. Niraj Luwang, R. Tewari, and R. K. Vatsa, Opt. Mater. **32**, 616 (2010).
[66]M. Yang, H. You, G. Jia, Y. Huang, Y. Song, Y. Zheng, K. Liu, and L. Zhang, J. Cryst. Growth **311**, 4753 (2009).
[67]S. Cotton, *Lanthanide and Actinide Chemistry, Inorganic Chemistry: A Textbook Series* (John Wiley & Sons, 2007), p. 14.
[68]T.-Ch. Huang, M.-T. Wang, H.-Sh. Sheu, and W.-F. Hsieh, J. Phys.: Condens. Matter **19**, 476212 (2007).